Proc. Roy. Soc. Lond. A. **319**, 247–272 (1970)
Printed in Great Britain

Elastic-plastic behaviour of polycrystalline metals and composites†

By J. W. Hutchinson
Harvard University,
Cambridge, Massachusetts

(*Communicated by R. Hill, F.R.S.—Received* 26 *March* 1970)

Stress–strain behaviour of polycrystals and composites is explored with self-consistent models based on the elastic-plastic properties of the single crystal constituents. Based on Hill's (1965*a*) model, tensile stress–strain curves and the associated yield surfaces are calculated for polycrystals and composites comprised of face-centred cubic crystals. Single crystal elastic anisotropy and strain hardening are taken into account. Stress–strain behaviour at a corner of the yield surface is determined with the model proposed by Kröner (1961) and Budiansky & Wu (1962).

1. Introduction

Many models have been proposed to predict both quantitative and qualitative features of the elastic-plastic behaviour of polycrystalline metals. Of principal concern here will be those based on the slip mechanism of the single crystal. One of the first of such theories was due to Taylor (1938) and extended by Bishop & Hill (1951) for the yielding of a polycrystal comprised of rigid-plastic single crystals. Another approach was pursued by Batdorf & Budiansky (1949). Their slip theory was an attempt to gain insight into elastic-plastic behaviour in the régime in which plastic strains are comparable in magnitude to elastic strains. Koiter (1953) and Sanders (1954) considered a very general class of plasticity theories, of which slip theory was a special case, based on the concept of many simultaneous yield surfaces.

More mechanistic models followed which specified ways to calculate stresses and strains in the individual crystals and to relate these to the overall stresses and strains of the polycrystal. Lin (1957) extended Taylor's model to include elastic strains. Budiansky, Hashin & Sanders (1960) made calculations based on a model which was valid for very small plastic strains relative to elastic strains; and Kröner (1961) and Budiansky & Wu (1962) proposed a model which accounted for grain interaction in a particular way and was not limited to very small plastic strains. This latter model specified a self-consistent method for calculating the overall stress–strain behaviour of the polycrystal. Calculations based on this model were made by Budiansky & Wu (1962) and Hutchinson (1964). A review of the efforts in this general problem area, with a strong emphasis on the underlying single crystal behaviour, has been given by Kocks (1970).

† This work was supported in part by the National Aeronautics and Space Administration under Grant NGL 22-007-012, in part by the Advanced Research Projects Agency under Contract SD-88, and by the Division of Engineering and Applied Physics, Harvard University.

The latest development in this subject is an attractive self-consistent model suggested by Hill (1965*a*). This new model is similar in a number of respects to the Kröner–Budiansky–Wu (K.B.W.) model but differs in the method proposed for calculating the stresses and strains in the individual grains. In two subsequent papers Hill (1966, 1967) elaborated on the description of single crystal behaviour and followed up with a very general qualitative discussion of the structure of the stress–stress relations expected from such a model.

One of the attractive features of Hill's model is that it embraces essentially all the accepted self-consistent results for the overall properties of elastic systems: see, for example, Hershey (1954) and Kröner's (1958) equations for the elastic moduli of cubic polycrystals, Kneer's (1963) results for hexagonal polycrystals, Budiansky (1965) and Hill's (1965*b*) formulas for the overall moduli of composites and Wu (1966) and Walpole's (1969) results for composites with shaped constituents.

In this paper a quantitative study of certain aspects of the elastic-plastic deformation of polycrystalline metals and composites is made using the two self-consistent models mentioned above. Primarily, however, attention is directed to Hill's model. Our study is restricted to small strain behaviour which takes place statically and isothermally in the range of deformation in which the plastic strains are comparable in magnitude to the elastic strains. Section 2 contains a summary presentation of the model as it applies here including a description of the properties of single crystals and their relationship to the overall properties of the polycrystal. Tensile stress–strain curves for face-centred cubic (f.c.c.) polycrystals are presented in §3 showing effects of elastic anisotropy and hardening of the crystals. A comparison of the various models is given in §4, and calculations which focus on the character of the yield surface and the stress–strain behaviour at a corner of the yield surface are given in §5. The last section includes an extension of the model to a class of inclusion-bearing composites and results in the form of tensile stress–strain curves are given. Major features of the numerical method are discussed in the appendix along with the presentation of an auxiliary elasticity solution required for implementation of the model.

2. Hill's self-consistent model of polycrystalline behaviour

For the most part we shall use the same abbreviated notation as Hill has used in each of his papers (1965*a*, *b*, 1966, 1967), which Walpole (1969) has also employed. Boldface lower case letters, Greek or Latin, are reserved as symbols for second-order Cartesian tensors and fourth-order Cartesian tensors are represented by boldface upper case symbols. The contracted product of two second-order tensors, $a_{ij}b_{ij}$, is written simply as $\boldsymbol{ab}$ while the second-order tensor formed by $A_{ijkl}a_{kl}$ is denoted by $\boldsymbol{Aa}$. Inner products between two fourth-order tensors, $A_{ijkl}B_{klmn}$, become $\boldsymbol{AB}$ in this notation and a scalar quantity $a_{ij}A_{ijkl}b_{kl}$ is denoted by $\boldsymbol{aAb}$.

In this paper all second-order tensors are symmetric; and except for the $\boldsymbol{S}$ tensor introduced in the Appendix, the symmetry $A_{ijkl} = A_{jikl} = A_{ijlk} = A_{klij}$ is shared by all fourth-order tensors. The inverse $\boldsymbol{A}^{-1}$ of $\boldsymbol{A}$ satisfies $\boldsymbol{A}^{-1}\boldsymbol{A} = \boldsymbol{A}\boldsymbol{A}^{-1} = \boldsymbol{I}$ where $\boldsymbol{I}$ is the 'unity tensor' whose components are given in terms of the Kronecker delta by

$$I_{ijkl} = \tfrac{1}{2}(\delta_{ik}\delta_{jl} + \delta_{il}\delta_{jk}). \tag{1}$$

Conversion of second-order tensors to column vectors and fourth-order tensors to symmetric matrices can be accomplished in several ways; and, if one prefers, the notation can be viewed as representing the usual vector-matrix operations.

(*a*) *Stress–strain behaviour for single crystals*

Idealizations of single crystal behaviour are based on the early work of Taylor & Elam (1923) together with the considerable experimental and theoretical work which has followed. Here plastic deformation is assumed to arise solely from slip in certain directions on specific crystallographic planes, and this process occurs when the resolved shear stress on one or more of these slip systems reaches a critical value. As plastic deformation proceeds the critical yield stresses associated with the slip systems can change, usually to raise the yield stresses so that the crystal 'hardens'. Budiansky & Wu (1962) emphasized that single crystal plasticity fits Koiter's (1960) continuum theory of plasticity involving multiple yield functions. Recently, Hill (1966) and Mandel (1965) have further pursued the constitutive relations for single crystals.

Let $\boldsymbol{\sigma}_c$ denote the stress in the crystal. If n_j^i is the normal to the plane of the ith slip system and if m_j^i is its slip direction, then the resolved shear stress on this system is $\sigma_{ckl}\alpha_{kl}^i$ or $\boldsymbol{\sigma}_c\boldsymbol{\alpha}^i$ in the present notation where

$$\alpha_{kl}^i = \tfrac{1}{2}(m_k^i n_l^i + m_l^i n_k^i) \quad \text{(no sum on } i\text{)}. \tag{2}$$

The plastic strain rate $\dot{\boldsymbol{\epsilon}}_c^p$ is the sum of the contributions of the shear rates $\dot{\gamma}^i$ (engineering definition) from all the active slip systems, i.e.

$$\dot{e}_{cij}^p = \sum_m \dot{\gamma}^m \alpha_{ij}^m \quad \text{or} \quad \dot{\boldsymbol{\epsilon}}_c^p = \sum_m \dot{\gamma}^m \boldsymbol{\alpha}^m. \tag{3}$$

We will adopt the convention that the yield stress and shear rate associated with each slip system is never negative and thereby, in effect, double the number of slip systems.

The current yield stress of the ith slip system is denoted by τ^i. At any stage of the deformation process the rates of change of the yield stresses are assumed to be related to the shear rates by (Hill 1966)

$$\dot{\tau}^i = \sum_j h^{ij}\dot{\gamma}^j, \tag{4}$$

where the instantaneous hardening coefficients h^{ij} will depend, in general, on the previous deformation history.

A slip system is potentially active if $\boldsymbol{\sigma}_c\boldsymbol{\alpha}^i = \tau^i$ and loads or unloads, respectively, depending on whether

$$\left.\begin{aligned} &\dot{\boldsymbol{\sigma}}_c\boldsymbol{\alpha}^i = \dot{\tau}^i \quad \text{with} \quad \dot{\gamma}^i \geqslant 0 \\ \text{or} \quad &\dot{\boldsymbol{\sigma}}_c\boldsymbol{\alpha}^i < \dot{\tau}^i \quad \text{with} \quad \dot{\gamma}^i = 0. \end{aligned}\right\} \tag{5}$$

A system is inactive if $\boldsymbol{\sigma}_c\boldsymbol{\alpha}^i < \tau^i$ and then $\dot{\gamma}^i = 0$.

Tensors of elastic moduli and compliance for the single crystal, $\mathscr{L}^c_{ijkl}$ and $\mathscr{M}^c_{ijkl}$, are denoted by $\mathscr{L}_c$ and $\mathscr{M}_c$ where $\mathscr{M}_c = \mathscr{L}_c^{-1}$. The total strain rate $\dot{\boldsymbol{\epsilon}}_c$ is the sum of the elastic and plastic parts so that

$$\dot{\boldsymbol{\epsilon}}_c = \mathscr{M}_c\dot{\boldsymbol{\sigma}}_c + \sum_i \dot{\gamma}^i\boldsymbol{\alpha}^i, \tag{6}$$

or

$$\dot{\boldsymbol{\sigma}}_c = \mathscr{L}_c(\dot{\boldsymbol{\epsilon}}_c - \dot{\boldsymbol{\epsilon}}^p_c). \tag{7}$$

For a given state of stress $\boldsymbol{\sigma}_c$, $\dot{\boldsymbol{\sigma}}_c$ is uniquely related to $\dot{\boldsymbol{\epsilon}}_c$ if h^{ij} is positive semi-definite (Hill 1966), while only for certain hardening laws are the shear rates $\dot{\gamma}^i$ always unique. At least one set of shear rates exists which satisfies the constitutive relations (3) to (7) for a prescribed strain rate $\dot{\boldsymbol{\epsilon}}_c$ (or prescribed $\dot{\boldsymbol{\sigma}}_c$). If there are N non-zero $\dot{\gamma}$'s, they satisfy N equations associated with the loading systems:

$$\sum_j \dot{\gamma}^j X^{ij} = \boldsymbol{\alpha}^i\mathscr{L}_c\dot{\boldsymbol{\epsilon}}_c, \tag{8}$$

where

$$X^{ij} = h^{ij} + \boldsymbol{\alpha}^i\mathscr{L}_c\boldsymbol{\alpha}^j, \tag{9}$$

together with the constraints $\dot{\gamma}^i \geqslant 0$.

Only for certain hardening laws will the N×N matrix X^{ij} be necessarily non-singular. But for perfect plasticity ($h^{ij} = 0$), for example, it is always possible to choose at least one set of linearly independent slip systems among the potentially active such that this matrix is non-singular and the auxiliary equations (5) are satisfied. Thus, for perfect plasticity X^{ij} is never greater than a 5×5 matrix. Its inverse is denoted by Y^{ij} and the N non-zero strain rates for this choice of active systems are given by

$$\dot{\gamma}^i = f^i\dot{\boldsymbol{\epsilon}}_c \quad \text{where} \quad f^i \equiv \sum_k Y^{ik}\mathscr{L}_c\boldsymbol{\alpha}^k. \tag{10}$$

The instantaneous moduli and compliances for the single crystal depend on the particular branch (i.e. set of active slip systems) which in turn depends on the prescribed $\dot{\boldsymbol{\epsilon}}_c$ (or $\dot{\boldsymbol{\sigma}}_c$). They relate $\dot{\boldsymbol{\sigma}}_c$ and $\dot{\boldsymbol{\epsilon}}_c$ by

$$\dot{\boldsymbol{\sigma}}_c = \boldsymbol{L}_c\,\dot{\boldsymbol{\epsilon}}_c \quad \text{and} \quad \dot{\boldsymbol{\epsilon}}_c = \boldsymbol{M}_c\dot{\boldsymbol{\sigma}}_c. \tag{11}$$

When the inverse of $\boldsymbol{L}_c$ exists $\boldsymbol{M}_c = \boldsymbol{L}_c^{-1}$, but in many instances it does not, such as for perfectly plastic crystals. When the inverse fails to exist, i.e. when $\boldsymbol{L}_c$ viewed as a matrix is singular, the stress rate $\dot{\boldsymbol{\sigma}}_c$ is restricted to certain regions in stress rate space. We will want to consider polycrystals of perfectly plastic single crystals and thus our treatment will emphasize the use of $\boldsymbol{L}_c$ rather than $\boldsymbol{M}_c$ since there is no restriction on the strain rate $\dot{\boldsymbol{\epsilon}}_c$. Using (7), (10) and (11), we find

$$\boldsymbol{L}_c = \mathscr{L}_c(\boldsymbol{I} - \sum_m \boldsymbol{\alpha}^m\boldsymbol{f}^{m'}), \tag{12}\dagger$$

† The prime on $\boldsymbol{f}^m$ is used to indicate that the terms $\boldsymbol{\alpha}^m\boldsymbol{f}^{m'}$ in (12) are fourth-order tensors formed by the uncontracted products $\alpha^m_{ij}f^m_{kl}$. It is a simple matter to show that $\boldsymbol{L}_c$ as given by (12) satisfies $L^c_{ijkl} = L^c_{klij}$ if $h^{ij} = h^{ji}$.

where the sum extends over all the loading slip systems. In summary $\boldsymbol{L}_c$ as given by (12) is unique for a given strain rate $\dot{\boldsymbol{\epsilon}}_c$ even if the shear rates $\dot{\gamma}^i$ are not. Of course, if all systems are inactive or unload the response is purely elastic and (12) reduces to $\boldsymbol{L}_c = \mathscr{L}_c$.

(*b*) *Overall stress–strain behaviour for the polycrystal*

Macroscopic stress and strain rates associated with the polycrystal are denoted by $\dot{\bar{\boldsymbol{\sigma}}}$ and $\dot{\bar{\boldsymbol{\epsilon}}}$ and their Cartesian components are taken to be the volume averages of the Cartesian components of the corresponding stress and strain rates in the single crystals. Hill (1967) has shown that this definition is rigorously consistent for a finite collection of single crystals under either a prescribed uniform surface traction over the boundary or a prescribed 'uniform straining' of the boundary surface. If the polycrystal comprises a sufficiently large number of crystals the distinction between these two ways of prescribing the loading is negligible. For conceptual simplicity we shall view the polycrystal as an infinite collection of single crystals subject to macroscopically homogeneous states of stress and strain.

Overall elastic moduli and compliances are denoted by $\mathscr{L}$ and $\mathscr{M}$ with $\mathscr{M} = \mathscr{L}^{-1}$. The instantaneous moduli and compliances in the plastic range relate the stress and strain rates by

$$\dot{\bar{\boldsymbol{\sigma}}} = \boldsymbol{L}\dot{\bar{\boldsymbol{\epsilon}}} \quad \text{and} \quad \dot{\bar{\boldsymbol{\epsilon}}} = \boldsymbol{M}\dot{\bar{\boldsymbol{\sigma}}}, \tag{13}$$

where $\boldsymbol{M} = \boldsymbol{L}^{-1}$ except when the inverse fails to exist. Just as for the single crystal, $\boldsymbol{L}$ and $\boldsymbol{M}$ will depend on the prescribed value of $\dot{\bar{\boldsymbol{\epsilon}}}$ (or $\dot{\bar{\boldsymbol{\sigma}}}$); but, unlike the corresponding single crystal moduli and compliances, they will not have only a finite number of branches. Instead, $\boldsymbol{L}$ and $\boldsymbol{M}$ will, in general, vary continuously as the direction of the prescribed strain (stress) rate varies in strain (stress) rate space; that is, $\boldsymbol{L}$ and $\boldsymbol{M}$ are homogeneous functions of degree zero of $\dot{\bar{\boldsymbol{\epsilon}}}$ (or $\dot{\bar{\boldsymbol{\sigma}}}$). Of course, if the stress rate–strain rate behaviour is thoroughly nonlinear (which the present model indicates as will be seen later), equations (13) do not define the instantaneous moduli and compliance tensors uniquely. For example, any $\boldsymbol{L}^0(\dot{\bar{\boldsymbol{\epsilon}}})$ for which $\boldsymbol{L}^0\dot{\bar{\boldsymbol{\epsilon}}} = 0$ for all $\dot{\bar{\boldsymbol{\epsilon}}}$ can be added to $\boldsymbol{L}$ and still yield the same relation between $\dot{\bar{\boldsymbol{\sigma}}}$ and $\dot{\bar{\boldsymbol{\epsilon}}}$. However, the nature of the Hill model is such that it does select a particular characterization for $\boldsymbol{L}$ and $\boldsymbol{M}$ among all the possibilities.

(*c*) *Self-consistent calculation of the overall instantaneous moduli*

Imagine that the polycrystal has undergone some definite history of straining and that the stress and potentially active slip systems in each single crystal are known. In this state the polycrystal is subject to an additional prescribed strain rate $\dot{\bar{\boldsymbol{\epsilon}}}$. Our objective is to calculate the stress and strain rates, $\dot{\boldsymbol{\sigma}}_c$ and $\dot{\boldsymbol{\epsilon}}_c$, as well as the instantaneous moduli $\boldsymbol{L}_c$ for each grain and to determine the polycrystalline quantities, $\dot{\bar{\boldsymbol{\sigma}}}$ and $\boldsymbol{L}$, as the appropriate averages over the grains. The model is most readily understood if, at this stage in the exposition, it is assumed that the active slip systems in each grain are known and thus that $\boldsymbol{L}_c$ is known for each grain.

Hill (1965*a*) proposed that the stress and strain rates in any individual crystalline grain be calculated in the following way. The shape and orientation of a particular

grain is approximated by a similarly alined ellipsoidal single crystal which is taken to be embedded in an infinite homogeneous matrix whose moduli $\boldsymbol{L}$ are the overall instantaneous moduli of the polycrystal to be determined. In this approximate way the interaction between the grain under consideration and its plastically deforming neighbours is taken into account. The stress and strain rates 'at infinity' in the matrix are identified with the macroscopic quantities $\dot{\bar{\boldsymbol{\sigma}}}$ and $\dot{\bar{\boldsymbol{\epsilon}}}$. Thus, the stress and strain rates in each grain are estimated by the solution to a problem in linear anisotropic elasticity. As Eshelby (1957) observed, the stress and strain rates in the ellipsoidal inclusion, $\dot{\boldsymbol{\sigma}}_c$ and $\dot{\boldsymbol{\epsilon}}_c$, will be uniform and can be related to the stress and strain rates at infinity by fourth order tensors $\boldsymbol{A}_c$ and $\boldsymbol{B}_c$ according to

$$\dot{\boldsymbol{\epsilon}}_c = \boldsymbol{A}_c \dot{\bar{\boldsymbol{\epsilon}}} \quad \text{and} \quad \dot{\boldsymbol{\sigma}}_c = \boldsymbol{B}_c \dot{\bar{\boldsymbol{\sigma}}} \tag{14}$$

and, where consistent with (13),

$$\boldsymbol{L}_c \boldsymbol{A}_c = \boldsymbol{B}_c \boldsymbol{L} \quad \text{and} \quad \boldsymbol{M}_c \boldsymbol{B}_c = \boldsymbol{A}_c \boldsymbol{M}. \tag{15}$$

Still following Hill, the calculation of $\boldsymbol{A}_c$ and $\boldsymbol{B}_c$ is facilitated by the introduction of a 'constraint' tensor $\boldsymbol{L}^*$ with inverse $\boldsymbol{M}^*$. These are defined by considering a matrix containing an ellipsoidal void with the same orientation and shape as the grain and subject to a traction rate, $\dot{\sigma}^*_{ij} n_j$, over the surface of the void where $\boldsymbol{n}$ is the inward unit normal to the void surface and $\dot{\boldsymbol{\sigma}}^*$ is constant. The associated uniform straining of the void $\dot{\boldsymbol{\epsilon}}^*$ is given by

$$\dot{\boldsymbol{\sigma}}^* = -\boldsymbol{L}^* \dot{\boldsymbol{\epsilon}}^* \quad \text{or} \quad \dot{\boldsymbol{\epsilon}}^* = -\boldsymbol{M}^* \dot{\boldsymbol{\sigma}}^*. \tag{16}$$

Defined in this manner, $\boldsymbol{L}^*$ and $\boldsymbol{M}^*$ depend only on $\boldsymbol{L}$ and the shape and orientation of the ellipsoid, and if the void is spherical, only on $\boldsymbol{L}$. Formulas for $\boldsymbol{L}^*$ for spherical voids are given in the appendix.

With the use of $\boldsymbol{L}^*$ and $\boldsymbol{M}^*$ the discrepancies between the stress and strain rates in a given single crystal inclusion and the rates in the matrix at infinity are related by

$$\dot{\bar{\boldsymbol{\sigma}}} - \dot{\boldsymbol{\sigma}}_c = -\boldsymbol{L}^* (\dot{\bar{\boldsymbol{\epsilon}}} - \dot{\boldsymbol{\epsilon}}_c) \quad \text{or} \quad \dot{\bar{\boldsymbol{\epsilon}}} - \dot{\boldsymbol{\epsilon}}_c = -\boldsymbol{M}^* (\dot{\bar{\boldsymbol{\sigma}}} - \dot{\boldsymbol{\sigma}}_c). \tag{17}$$

Now, using (11), (13) and (17) we find

$$(\boldsymbol{L}^* + \boldsymbol{L}_c)\dot{\boldsymbol{\epsilon}}_c = (\boldsymbol{L}^* + \boldsymbol{L})\dot{\bar{\boldsymbol{\epsilon}}} \quad \text{and} \quad (\boldsymbol{M}^* + \boldsymbol{M}_c)\dot{\boldsymbol{\sigma}}_c = (\boldsymbol{M}^* + \boldsymbol{M})\dot{\bar{\boldsymbol{\sigma}}}, \tag{18}$$

or by the defining equations (14),

$$\boldsymbol{A}_c = (\boldsymbol{L}^* + \boldsymbol{L}_c)^{-1}(\boldsymbol{L}^* + \boldsymbol{L}) \quad \text{and} \quad \boldsymbol{B}_c = (\boldsymbol{M}^* + \boldsymbol{M}_c)^{-1}(\boldsymbol{M}^* + \boldsymbol{M}). \tag{19}$$

The final step in the formulation equates the overall stress and strain rates of the polycrystal with the weighted averages of these same quantities over all the grain orientations and shapes. For a particular grain $\dot{\boldsymbol{\sigma}}_c = \boldsymbol{L}_c \boldsymbol{A}_c \dot{\bar{\boldsymbol{\epsilon}}}$; and if the average over all the grains is denoted by $\{\ \}$, then

$$\{\dot{\boldsymbol{\sigma}}_c\} = \dot{\bar{\boldsymbol{\sigma}}} \Rightarrow \boldsymbol{L} = \{\boldsymbol{L}_c \boldsymbol{A}_c\}. \tag{20}$$

Similarly,

$$\{\dot{\boldsymbol{\epsilon}}_c\} = \dot{\bar{\boldsymbol{\epsilon}}} \Rightarrow \boldsymbol{M} = \{\boldsymbol{M}_c \boldsymbol{B}_c\}. \tag{21}$$

The derivation of (21), but not (20), requires the inverse of L_c for each grain to exist. When this requirement is satisfied, (20) and (21) are on an equal footing and Hill (1965) has emphasized that they lead to identical results as can be seen directly with the aid of (15). As already mentioned, we will make use of L_c together with (20) and avoid the difficulties associated with (21) when any of the L_c are singular.

In the foregoing discussion it was assumed that the branch of L_c for each grain for a prescribed overall strain rate $\dot{\mathbf{E}}$ was known, whereas the actual branch depends on the strain rate $\dot{\boldsymbol{\epsilon}}_c$ in each grain. Thus, (20) governing the overall instantaneous moduli is supplemented by the requirement that the branch of L_c for each grain be that associated with the predicted value of $\dot{\boldsymbol{\epsilon}}_c$ from (14).

(*d*) *Spherical grain model applied to a polycrystal of randomly orientated f.c.c. single crystals*

In this paper stresses and strains in individual grains will be calculated by approximating each grain by a sphere. Furthermore, all grain orientations will be assumed equally represented and thus an average over all grains is equivalent to an average over all orientations.

The tensor of overall elastic moduli, $\mathscr{L}$, for such a polycrystal is a fourth-order isotropic tensor specified by its bulk modulus κ and its shear modulus μ. Hershey (1954) and Kröner's (1958) equations for these quantities for a cubic polycrystal are

$$\kappa = \tfrac{1}{3}(C_{11}+2C_{12}) \tag{22}$$

$$8\mu^3+(5C_{11}+4C_{12})\mu^2-C_{44}(7C_{11}-4C_{12})\mu-C_{44}(C_{11}-C_{12})(C_{11}+2C_{12}) = 0, \tag{23}$$

where C_{11}, C_{12} and C_{44} are the three independent elastic constants defined in the usual way for a cubic crystal. These equations can be derived from either (20) or (21) as discussed in the appendix.

A f.c.c. crystal has 12 crystallographically similar slip systems (24 systems with our convention, $\dot{\gamma} \geqslant 0$) whose normals are the four (1, 1, 1)-type directions, relative to the crystal axes, and whose slip directions are the (1, 1, 0)-type directions. If the single crystals are elastically isotropic with an initial yield stress τ_y^0 associated with each slip system, the stress will be uniform throughout the polycrystal prior to yield. Since all slip system orientations are available, initial yield will be governed by the maximum shear stress, or Tresca, criterion, assuming no residual stresses are present. The Tresca criterion still holds for a polycrystal of anisotropic cubic crystals according to a self-consistent calculation based on spherical grains.

If $\bar{\sigma}_{\mathrm{I}}$ and $\bar{\sigma}_{\mathrm{III}}$ are the maximum and minimum principal overall stresses, respectively, the macroscopic initial yield condition is given in terms of the initial yield stress of the crystals τ_y^0 by

$$\tfrac{1}{2}|\bar{\sigma}_{\mathrm{I}}-\bar{\sigma}_{\mathrm{III}}| = \left(\frac{3}{2\rho_2^2+\rho_3^2}\right)^{\frac{1}{2}}\tau_y^0 \equiv \bar{\tau}_y^0, \tag{24}$$

where

$$\rho_2 = \frac{C_{11}-C_{12}}{2\mu(1-\beta)+\beta(C_{11}-C_{12})}, \quad \rho_3 = \frac{C_{44}}{\mu(1-\beta)+\beta C_{44}}, \tag{25}$$

$$\beta = \frac{6}{5}\left(\frac{\kappa + 2\mu}{3\kappa + 4\mu}\right), \tag{26}$$

and where κ and μ are given by (22) and (23). If the single crystals are isotropic, i.e. $2C_{44} = C_{11} - C_{12}$, then $\rho_2 = \rho_3 = 1$ and $\overline{\tau}_y^0 = \tau_y^0$ as mentioned above. The effect of grain size on initial yield is encompassed by the model only to the extent that τ_y^0 must be regarded as the yield stress of the single crystal *in situ*. Details of the derivation of this result are given in the appendix and a discussion of some of its implications and limitations is given in the next section.

Behaviour in the plastic range is complex and predictions require numerical calculations. For example, (20) is a highly implicit equation for the instantaneous moduli $\boldsymbol{L}$ involving $\boldsymbol{L}^*$, which is a function of $\boldsymbol{L}$, and the instantaneous moduli of each of the grains $\boldsymbol{L}_c$. Moreover, the particular branch of $\boldsymbol{L}_c$ is related in a very complicated way to $\boldsymbol{L}$ and the prescribed overall stress or strain rate, $\dot{\boldsymbol{\sigma}}$ or $\dot{\boldsymbol{\epsilon}}$. A bare outline of the numerical procedure follows and is further elaborated on in the appendix.

At a given stage in calculation the stresses and the potentially active slip systems in each of the spherical grains are known. We wish to calculate the stress or strain rates and instantaneous moduli for a prescribed overall stress rate $\dot{\boldsymbol{\sigma}}$ or a prescribed overall strain rate $\dot{\boldsymbol{\epsilon}}$. The procedure is an iterative one. A tentative guess is made for $\boldsymbol{L}$, and $\boldsymbol{L}^*$ is calculated. From $\boldsymbol{L}$ and $\boldsymbol{L}^*$ the instantaneous moduli for each grain orientation are computed in the following way. For an assumed set of active (loading) slip systems, necessarily a subset of the potentially active systems, the quantities f^i of (10) are calculated and so is $\boldsymbol{L}_c$ from (12). Next $\boldsymbol{A}_c$ is calculated for this grain with (19). To ensure that the assumed set of active slip systems do constitute the correct branch of $\boldsymbol{L}_c$ for a prescribed $\dot{\boldsymbol{\epsilon}}$ (or $\dot{\boldsymbol{\sigma}}$), the auxiliary conditions (5) are checked with (4), (10), (11) and (14). If conditions (5) are satisfied then $\boldsymbol{L}_c$ is correct for this iteration; if not, then a new set of active slip systems is chosen until the correct $\boldsymbol{L}_c$ and $\boldsymbol{A}_c$ are found. This calculation is carried out for each grain orientation. The final step in the first iteration is to calculate an improved estimate for $\boldsymbol{L}$ from $\boldsymbol{L} = \{\boldsymbol{L}_c \boldsymbol{A}_c\}$. The whole procedure is then repeated a sufficient number of times until satisfactory convergence is obtained.

A complete deformation history for a prescribed history of overall stress or strain is calculated in a piecewise linear manner with finite but small increments. As the deformation proceeds new slip systems are activated while other slip systems which were active unload.

3. Tensile stress–strain relations for f.c.c. polycrystals

Let the virgin polycrystal be subject to a monotonically increasing uniaxial tensile stress $\overline{\sigma}_{33} \equiv \sigma$. The instantaneous moduli for this history display transverse isotropy with respect to the 3-axis so that with the usual definition

$$\dot{\overline{\sigma}}_i = L_{ij}\dot{\overline{\epsilon}}_j \quad \text{and} \quad \dot{\overline{\epsilon}}_i = M_{ij}\dot{\overline{\sigma}}_j \quad (\text{sum on } j;\, j = 1, 6), \tag{27}$$

where
$$\dot{\bar{e}}_i \Leftrightarrow (\dot{\bar{e}}_{11}, \dot{\bar{e}}_{22}, \dot{\bar{e}}_{33}, 2\dot{\bar{e}}_{13}, 2\dot{\bar{e}}_{23}, 2\dot{\bar{e}}_{12}),$$
$$\dot{\bar{\sigma}}_i \Leftrightarrow (\dot{\bar{\sigma}}_{11}, \dot{\bar{\sigma}}_{22}, \dot{\bar{\sigma}}_{33}, \dot{\bar{\sigma}}_{13}, \dot{\bar{\sigma}}_{23}, \dot{\bar{\sigma}}_{12}).$$

The non-zero independent moduli are

$$L_{ij} = \begin{bmatrix} L_{11} & L_{12} & L_{13} & 0 & 0 & 0 \\ L_{12} & L_{11} & L_{13} & 0 & 0 & 0 \\ L_{13} & L_{13} & L_{33} & 0 & 0 & 0 \\ 0 & 0 & 0 & L_{44} & 0 & 0 \\ 0 & 0 & 0 & 0 & L_{44} & 0 \\ 0 & 0 & 0 & 0 & 0 & L_{66} \end{bmatrix}, \tag{28}$$

where $L_{66} = \frac{1}{2}(L_{11} - L_{12})$.

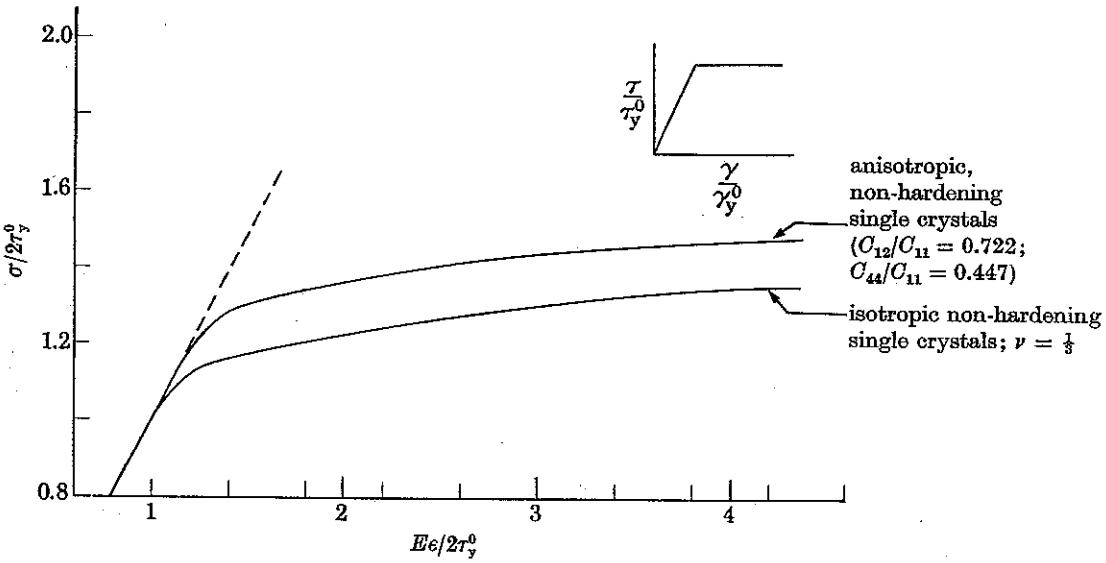

FIGURE 1. Tensile stress–strain curves for f.c.c. polycrystals with randomly orientated, non-hardening single crystals. Upper curve is for anistropy typical of copper.

The initial yield stress in tension according to this model is $2\bar{\tau}_y^0$ where $\bar{\tau}_y^0$ is given by (24). If the single crystals are isotropic then $\bar{\tau}_y^0 = \tau_y^0$, the initial yield stress associated with each slip system. Typically, for copper, which in crystal form has moderately high elastic anisotropy: $(C_{12}/C_{11}) = 0.722$ and $(C_{44}/C_{11}) = 0.447$; and the self-consistent predictions from (22), (23) and (24) are

$$\kappa = 0.815C_{11}, \quad \mu = 0.285C_{11}, \quad \bar{\tau}_y^0 = 1.129\tau_y^0 \tag{29}$$

or
$$E = 0.772C_{11}, \quad \nu = 0.343,$$

where E and ν are the Young modulus and Poisson ratio, respectively.

Tensile stress–strain curves are presented in figure 1 for polycrystals of non-hardening single crystals which are (i) isotropic with Young's modulus E and $\nu = \frac{1}{3}$ and (ii) anisotropic with the moduli ratios of copper just listed. The ordinate is the

ratio $\sigma/2\tau_y^0$ and the abscissa is $E\epsilon/2\tau_y^0$ where ϵ is the total tensile strain. Thus, in this plot the elastic part of each curve has the same slope and the increase in the initial yield stress for the copper-like anisotropy above that of the isotropic case is evident.

The initial yield prediction of the self-consistent model must be qualified. A non-homogeneity in an elastic body usually acts as a stress raiser and tends to decrease, rather than increase, the stress at which plastic deformation first occurs. Single crystal anisotropy would be expected to have a similar effect; but according to the self-consistent model based on the spherical grain, it does not if

$$2C_{44} > (C_{11} - C_{12}).$$

The reason for this stems from the fact that stresses in each grain are calculated by treating it as a spherical inclusion. Stresses in the matrix surrounding the inclusion do not enter into the self-consistent estimate of initial yield. No doubt highly

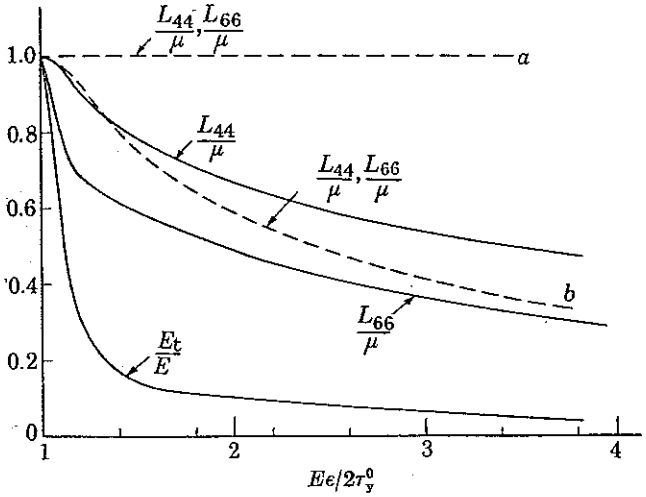

FIGURE 2. Several instantaneous moduli as a function of the tensile strain for a polycrystal with isotropic non-hardening single crystals ($\nu = \frac{1}{3}$) and comparisons with predictions of two phenomenological theories: *a*, flow theory with smooth yield surface; *b*, deformation theory.

localized plastic deformation will occur in the polycrystal at tensile stresses even below $2\tau_y^0$ when the crystals are anisotropic, but the value $2\tau_y^0$ should serve as an effective measure of the tensile stress at which plastic strain starts to increase rapidly. An even clearer illustration of this limitation of the self-consistent model is discussed in a later section on composite materials.

Figure 2 contains plots of three of the components of the instantaneous moduli as a function of the tensile strain for a polycrystal with non-hardening isotropic crystals. The so-called tangent modulus, $E_t \equiv \mathrm{d}\sigma/\mathrm{d}\epsilon$, where

$$E_t = \frac{1}{M_{33}} = L_{33} - \frac{2L_{13}^2}{L_{11} + L_{12}}$$

is normalized by the Young modulus E, while L_{44} and L_{66} are each normalized by their elastic value, the modulus μ. The moduli L_{44} and L_{66} can be compared with predictions from two popular phenomenological theories. According to any flow (incremental) theory of plasticity with a smooth yield surface $L_{44} = L_{66} = \mu$ for any tensile history and this prediction is included in figure 2. Also shown, as a dashed curve, is the prediction obtained from any deformation theory where L_{44} and L_{66} are derived from the tensile stress–strain curve using the deformation theory formula

$$L_{44} = L_{66} = \frac{\mu}{1 + 3\mu\left(\frac{1}{E_s} - \frac{1}{E}\right)}, \tag{30}$$

where $E_s \equiv \sigma/e$.

No entirely adequate hardening law for single crystals is available. Taylor's (1938) isotropic hardening law is the simplest and the most widely used. This law states that the yield stresses of all slip systems remain equal and increase in proportion to the total shear. So that in (4), $h^{ij} = h$ for all i and j, and

$$\dot{\tau}^i = h\sum_j \dot{\gamma}^j. \tag{31}$$

This rule cannot include both the very low hardening rate characteristic of easy glide with one slip system active *and* the much higher hardening rate which usually accompanies multiple slip, as discussed by Kocks (1970). Nor does it reflect the experimental observation that some of the latent slip systems usually harden faster than active ones.

Another candidate, which is only slightly more complicated than Taylor's rule qualitatively, at least, meets these two objections. It is

$$h^{ij} = h_m + (h_s - h_m)\delta^{ij}, \tag{32}$$

where h_s is to be identified with the hardening rate for single slip and h_m to characterize multiple slip. Hill (1966) has remarked that (32) as well as (31) will lead, in general, to non-unique shear rates $\dot{\gamma}^i$ for prescribed stress or strain rates $\dot{\boldsymbol{\sigma}}_c$ or $\dot{\boldsymbol{\epsilon}}_c$. Neither (31) or (32) includes a single crystal Bauschinger effect but this is of little concern in deriving macroscopic predictions as long as no reverse loading histories are considered.

We have steered clear of the inadequacy of single crystal hardening laws and have only calculated results for the stress–strain behaviour in the fairly early stages of plastic deformation. The tensile stress-plastic strain curves plotted in figure 3 are representative of the way crystal hardening affects overall hardening of the polycrystal. In this plot e^p is the tensile plastic strain. These curves have been calculated with Taylor's rule (31) with a relatively light hardening rate $h/\mu = 0.02$ and a somewhat higher value $h/\mu = 0.04$. The non-hardening case ($h/\mu = 0$) is repeated from figure 1.

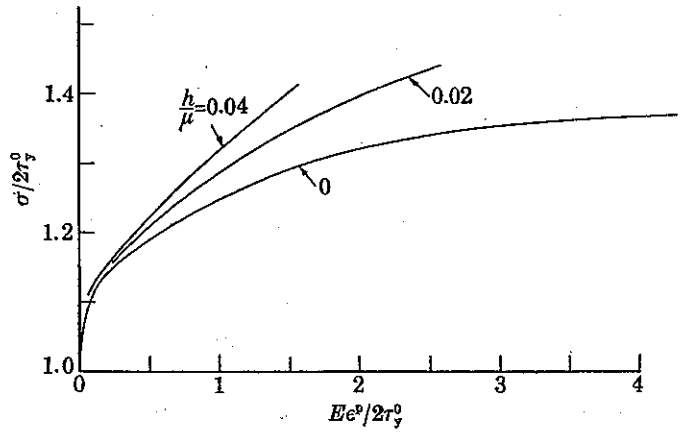

FIGURE 3. Effect of single crystal hardening on tensile stress–plastic strain curves. Isotropic single crystals, $\nu = \frac{1}{3}$. Taylor hardening: $\tau_y = \tau_y^0 + h\Sigma\gamma^i$.

4. COMPARISONS WITH OTHER MODELS

The self-consistent model of Kröner (1961) and Budiansky & Wu (1962) fits nicely into the theoretical structure that Hill has constructed. Instead of embedding the grain in a matrix whose moduli are the overall instantaneous moduli, Kröner and Budiansky & Wu argue that the relation

$$\dot{\boldsymbol{\sigma}} - \dot{\boldsymbol{\sigma}}_c = -\mathscr{L}^*(\dot{\bar{\boldsymbol{\epsilon}}} - \dot{\boldsymbol{\epsilon}}_c), \tag{33}$$

which holds in the elastic range also holds in the plastic range, and this replaces (17). Here, $\mathscr{L}^*$ is the constant tensor, previously defined, for a matrix with overall isotropic elastic moduli $\mathscr{L}$. This leads to

$$\boldsymbol{A}_c = (\mathscr{L}^* + \boldsymbol{L}_c)^{-1}(\mathscr{L}^* + \boldsymbol{L}) \quad \text{and} \quad \boldsymbol{B}_c = (\mathscr{M}^* + \boldsymbol{M}_c)^{-1}(\mathscr{M}^* + \boldsymbol{M}) \tag{34}$$

rather than (19), while the remaining equations in §2 still apply.

Figure 4 compares tensile stress–plastic strain curves for the two models for a polycrystal of randomly orientated, isotropic single crystals with no hardening. In the early stages of plastic deformation the predictions of the Hill model and the K.B.W. model are essentially identical since then $\boldsymbol{L}^*$ in (19) is approximately $\mathscr{L}^*$ which appears in (34). However, as plastic deformation increases, the overall instantaneous moduli $\boldsymbol{L}$ decrease and so do the components of $\boldsymbol{L}^*$. Thus, the matrix surrounding each grain is considerably weakened in the Hill model, compared to the K.B.W. model, and consequently the plastic strain rate is greater for the Hill model at a given value of the tensile stress. Plots of instantaneous moduli calculated from the K.B.W. model are qualitatively very similar to those of figure 2 for the Hill model.

As long as only a small fraction of the grains have yielded, a 'dilute' calculation is applicable in which each yielded grain is considered to be embedded in a matrix whose moduli are those of the elastic polycrystal. The K.B.W. and Hill models

reduce to this limit, and in the *very early stages* of plastic deformation predictions based on them are essentially the same as those of Budiansky *et al.* (1960). The range of validity of a dilute calculation is very small, however. For example, slip is under way in over half of the grains at an overall plastic tensile strain of only 5 % of the initial tensile yield strain.

Predictions from Lin's (1957) extension to Taylor's model are also included in figure 4. Lin assumed that the strain is uniform throughout the polycrystal even when the elastic strains are not negligible. Thus, $A_c = I$ and $L = \{L_c\}$. This suggestion was not intended to be self-consistent. Furthermore, as discussed by Hutchinson (1964), the plastic strain according to Lin's model is exactly $\frac{8}{15}$ths the plastic strain predicted by the K.B.W. model at a given value of the tensile stress for $\nu = \frac{1}{3}$.

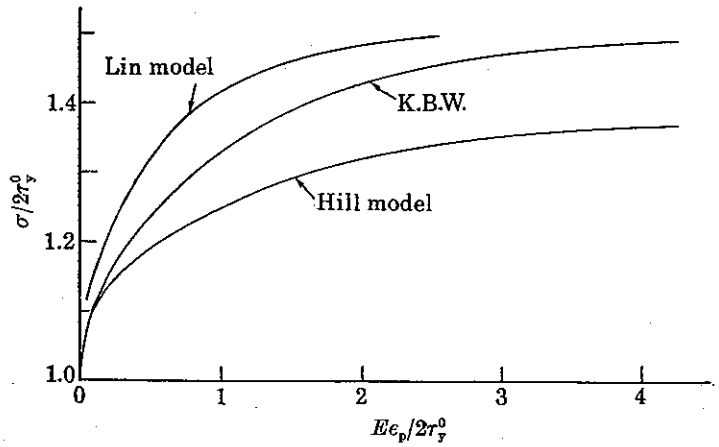

FIGURE 4. Comparison of theoretical tensile stress–plastic strain curves for f.c.c. polycrystals. Isotropic, non-hardening single crystals, $\nu = \frac{1}{3}$.

The limit yield surface for polycrystals of non-hardening crystals according to both the K.B.W. and the Lin models is precisely that calculated by Bishop & Hill (1951) for f.c.c. metals and by Hutchinson (1964) for b.c.c. metals. No such simple relation is evident for Hill's model; but, as discussed by Hill (1967), the previously mentioned limit yield surfaces serve as upper bounds. Figure 1 suggests that the limit yield stress in tension according to Hill's model may be somewhat lower than Taylor's tensile limit and may depend on the degree of elastic anisotropy of the single crystals, although it is possible that at larger strains the discrepancies between the two curves will disappear.

5. THE POLYCRYSTALLINE YIELD SURFACE AND STRESS–STRAIN BEHAVIOUR AT A CORNER

An immediate consequence of the results for the instantaneous moduli plotted in figure 2 is that the polycrystalline yield surface develops a corner after only a very small amount of plastic deformation. For, if the yield surface remained smooth,

then necessarily $L_{44} = L_{66} = \mu$. Previous studies based on slip theory, as well as Hill's (1967) general discussion of the present and related models, suggested corners should indeed be expected.

Corners are brought out clearly in the plots in figure 5 of the initial and subsequent yield surfaces as predicted by Hill's model. Shown are traces of the yield surface on two planes in stress-space, i.e. $\bar{\sigma}_{33}$ against $\bar{\sigma}_{13}$ and $\bar{\sigma}_{33}$ against $\bar{\sigma}_{12}$, at several values of the tensile stress. As discussed in § 2, the Tresca condition specifies the *initial* yield surface. The subsequent yield surfaces are for the polycrystal of isotropic non-hardening crystals whose tensile stress–strain curve is given in figures 1 and 3. No single crystal Bauschinger effect was incorporated into the calculations and thus the Bauschinger effect which is evident in figure 5 is due entirely to grain interaction effects. Yield surfaces predicted by the K.B.W. model are very similar to those shown in figure 5 and tensile stress–strain curves under fully reversed loading histories have been given for the K.B.W. model by Hutchinson (1964).

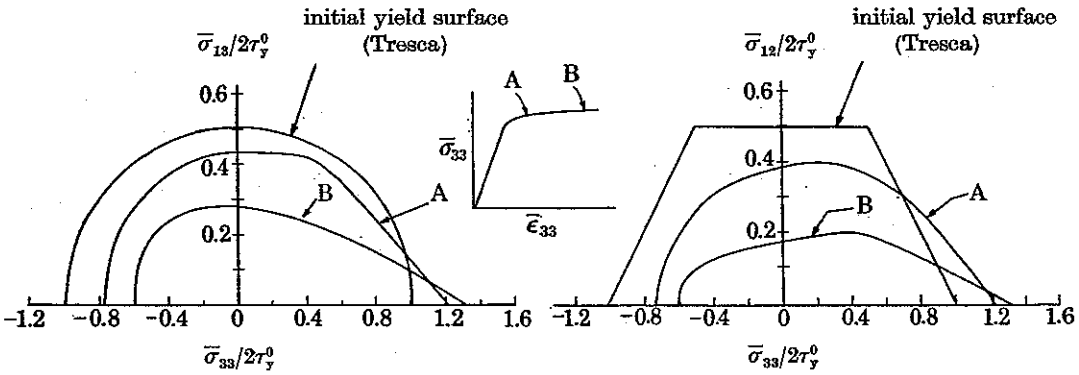

FIGURE 5. Initial and subsequent yield surfaces for the tensile deformation of an f.c.c polycrystal comprised of isotropic ($\nu = \frac{1}{3}$), non-hardening crystals.

Crystal hardening behaviour will influence the shape of the subsequent yield surfaces. If the tendency for latent slip systems to harden more rapidly than active systems is accounted for as well as the crystal Bauschinger effect, the yield surface will contract less in directions in stress space which are normal to the direction of loading and it will contract more in the direction opposite to the loading direction.

To explore the stress–strain behaviour at the corner, we consider the application of a non-uniaxial stress rate in the form of a combination of $\dot{\bar{\sigma}}_{13}$ and $\dot{\bar{\sigma}}_{33}$ following a uniaxial history to the stress level $\bar{\sigma}_{33}$. The instantaneous moduli for this applied stress rate no longer possess transverse isotropy. With the same definition as in (27), two of the strain rates, $\dot{\bar{\epsilon}}_{33}$ and $\dot{\bar{\epsilon}}_{13}$, are related to the non-zero applied stress rates $\dot{\bar{\sigma}}_{33}$ and $\dot{\bar{\sigma}}_{13}$ by

$$\dot{\bar{\epsilon}}_{33} = M_{33}\dot{\bar{\sigma}}_{33} + M_{34}\dot{\bar{\sigma}}_{13},$$

$$2\dot{\bar{\epsilon}}_{13} = M_{43}\dot{\bar{\sigma}}_{33} + M_{44}\dot{\bar{\sigma}}_{13},$$

where $M_{43} = M_{34}$. The effective shear modulus associated with this programme of loading is the quantity usually measured in experiments. It is defined by

$$\mu_e \equiv \frac{\dot{\bar{\sigma}}_{13}}{2\dot{\bar{\epsilon}}_{13}} = \frac{1}{M_{44} + M_{34}(\dot{\bar{\sigma}}_{33}/\dot{\bar{\sigma}}_{13})}.$$

Instantaneous moduli and compliances along with μ_e have been calculated for the full range of combinations of $\dot{\bar{\sigma}}_{13}$ and $\dot{\bar{\sigma}}_{33}$, and also for combinations of $\dot{\bar{\sigma}}_{12}$ and $\dot{\bar{\sigma}}_{33}$, for a polycrystal of isotropic non-hardening f.c.c. crystals initially stressed to a value $(\bar{\sigma}_{33}/2\tau_y^0) = 1.30$ with the associated tensile strain $(E\epsilon/2\tau_y^0) = 2.13$. These calculations were carried out using the K.B.W. model rather than the Hill model because the

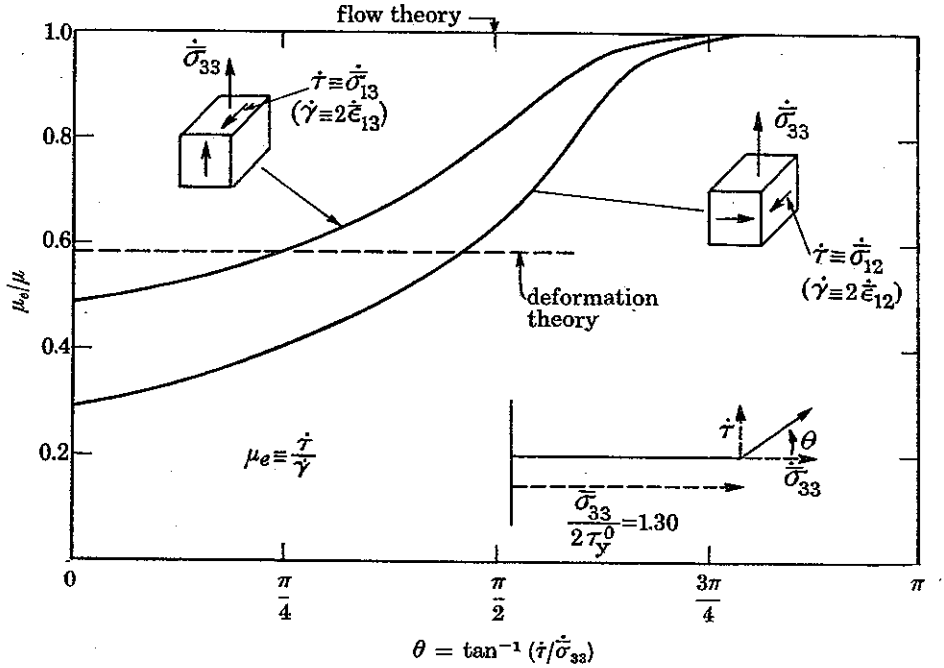

FIGURE 6. Effective shear modulus for combinations of $(\dot{\bar{\sigma}}_{13}, \dot{\bar{\sigma}}_{33})$ or $(\dot{\bar{\sigma}}_{12}, \dot{\bar{\sigma}}_{33})$ following a uniaxial stress $\bar{\sigma}_{33}$. Calculations are based on the K.B.W. model for polycrystals of isotropic ($\nu = \frac{1}{3}$), non-hardening single crystals.

L^* calculation necessary for the Hill model becomes considerably more difficult in the absence of transverse isotropy. Some of the details of the calculation are spelled out in the appendix. Qualitatively, at least, the results can be expected to be very similar to analogous predictions based on the Hill model.

Figure 6 displays a plot of μ_e/μ as a function of $\theta = \tan^{-1}(\dot{\bar{\sigma}}_{13}/\dot{\bar{\sigma}}_{33})$. A corresponding plot for the combination of stress rates $(\dot{\bar{\sigma}}_{12}, \dot{\bar{\sigma}}_{33})$ is also given with $\mu_e \equiv \dot{\bar{\sigma}}_{12}/2\dot{\bar{\epsilon}}_{12}$. Three compliances associated with the applied stress rates $(\dot{\bar{\sigma}}_{13}, \dot{\bar{\sigma}}_{33})$ are plotted as a function of θ in figure 7. Here M_{34} and M_{44} have been nondimensionalized by the elastic shear modulus μ, and E_t is used to nondimensionalize M_{33} where as previously defined $E_t = (1/M_{33})_{\theta=0}$.

According to these self-consistent results the effective shear modulus is appreciably reduced below the elastic value and only for θ greater than about $\frac{3}{4}\pi$ will the response be purely elastic. For $\theta \leqslant \frac{1}{2}\pi$, say, the prediction of deformation theory does reflect a reduction of the effective shear modulus, while flow theory with a smooth yield surface does not. It is this distinction between these two phenomenological theories which often leads to rather critical discrepancies in the application of these theories to the analysis of bifurcation phenomena such as buckling.

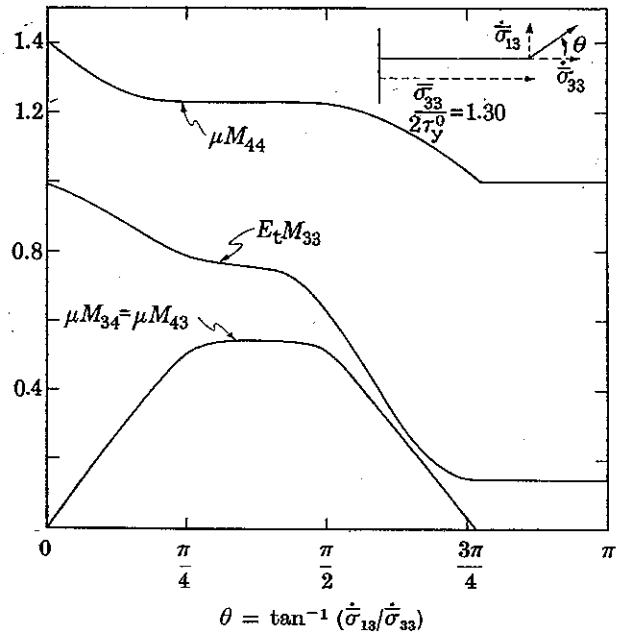

FIGURE 7. Instantaneous compliances for combinations of $(\dot{\bar{\sigma}}_{13}, \dot{\bar{\sigma}}_{33})$ following a uniaxial stress $\bar{\sigma}_{33}$. Calculations are based on the K.B.W. model for polycrystals of isotropic ($\nu = \frac{1}{3}$), non-hardening single crystals. $\dot{\bar{\epsilon}}_{33} = M_{33}\dot{\bar{\sigma}}_{33} + M_{34}\dot{\bar{\sigma}}_{13}$, $2\dot{\bar{\epsilon}}_{13} = M_{43}\dot{\bar{\sigma}}_{33} + M_{44}\dot{\bar{\sigma}}_{13}$.

Note that the effective shear modulus for a nearly proportional application of the stress rates $(\dot{\bar{\sigma}}_{13}, \dot{\bar{\sigma}}_{33})$, i.e. $\theta \approx 0$, is *not* given simply by $\mu_e = 1/M_{44}$ since the term $M_{34}(\dot{\bar{\sigma}}_{33}/\dot{\bar{\sigma}}_{13})$ in the foregoing formula contributes in the limit as $\theta \to 0$; and μ_e is less than $1/M_{44}$. It is also interesting to note that the effective shear modulus associated with the combination of stress rates $(\dot{\bar{\sigma}}_{13}, \dot{\bar{\sigma}}_{33})$, which is much more convenient to measure experimentally than μ_e associated with $(\dot{\bar{\sigma}}_{12}, \dot{\bar{\sigma}}_{33})$, is reduced less below the elastic value.

Experimental evidence on the existence of corners and the associated effective moduli is not conclusive and to a certain extent is actually contradictory. Hill (1967) has briefly reviewed the status of the test results relating to this equation. It seems reasonable to say that more tests will be required to improve the present unclear state of affairs. No doubt the precise properties of the crystals will play an important role in determining the quantitive values of the moduli at a corner. It is

clear from the self-consistent model, for example, that single crystal hardening will tend to bring the effective shear modulus closer to the elastic value. Nevertheless, self-consistent models based on single crystal slip, like their predecessor, slip theory, unequivocally indicate that a distinct corner develops as the polycrystal is deformed plastically.

The elastic-plastic behaviour displayed in figures 6 and 7 is thoroughly nonlinear in Hill's (1967) terminology. Slip theory results (Batdorf & Budiansky 1949; Sanders 1954) have suggested that for nearly proportional loading the stress–strain behaviour should be 'total', that is, independent of θ. While these self-consistent results do not corroborate the total loading concept exactly, the effective shear and tensile moduli do vary rather slowly for $\theta \approx 0$.

6. Application of the spherical grain self-consistent model to two-phase f.c.c. composites

Our objective as far as composites are concerned will be a short preliminary study to display the type of results that can be expected from an application of the self-consistent approach to elastic–plastic composite systems. This approach has been discussed extensively in the purely elastic context by Budiansky (1965), Hill (1965*b*) and Walpole (1969). Hill's (1967) general discussion of the essential structure of elastic–plastic behaviour pertains to composites as well as polycrystals.

The formulas for a two-phase composite are straightforward generalizations of those given in §2. Stresses and strains in every grain of each constituent are calculated 'individually' by replacing the grain under consideration by an equivalently alined ellipsoid which is embedded in a homogeneous matrix whose instantaneous moduli $\boldsymbol{L}$ are the desired overall moduli of the composite (for a prescribed overall stress or strain rate). The macroscopic moduli are given as the appropriate averages of the instantaneous properties of the grains in an obvious generalization of (20) and (21):

$$\boldsymbol{L} = c_1\{\boldsymbol{L}_c^{(1)}\boldsymbol{A}_c^{(1)}\} + c_2\{\boldsymbol{L}_c^{(2)}\boldsymbol{A}_c^{(2)}\}, \quad \boldsymbol{M} = c_1\{\boldsymbol{M}_c^{(1)}\boldsymbol{B}_c^{(1)}\} + c_2\{\boldsymbol{M}_c^{(2)}\boldsymbol{B}_c^{(2)}\}, \tag{35}$$

where c_1 is the volume fraction of phase 1 whose moduli are $\boldsymbol{L}_c^{(1)}$ and similarly for c_2 and $\boldsymbol{L}_c^{(2)}$. For the ith phase:

$$\dot{\boldsymbol{\epsilon}}_c^{(i)} = \boldsymbol{A}_c^{(i)}\dot{\bar{\boldsymbol{\epsilon}}}, \quad \dot{\boldsymbol{\sigma}}_c^{(i)} = \boldsymbol{B}_c^{(i)}\dot{\bar{\boldsymbol{\sigma}}} \tag{36}$$

and

$$\boldsymbol{A}_c^{(i)} = (\boldsymbol{L}^* + \boldsymbol{L}_c^{(i)})^{-1}(\boldsymbol{L}^* + \boldsymbol{L}), \quad \boldsymbol{B}_c^{(i)} = (\boldsymbol{M}^* + \boldsymbol{M}_c^{(i)})^{-1}(\boldsymbol{M}^* + \boldsymbol{M}). \tag{37}$$

As in the previous sections, calculations will be based on the assumption that the grains of each phase can be represented by spherical inclusions and that neither phase has a preferred orientation. In the elastic range such a composite will be macroscopically isotropic. The following coupled equations govern its bulk and shear moduli, κ and μ:

$$1 = c_1\rho_1^{(1)} + c_2\rho_1^{(2)}, \quad 5 = 2(c_1\rho_2^{(1)} + c_2\rho_2^{(2)}) + 3(c_1\rho_3^{(1)} + c_2\rho_3^{(2)}). \tag{38}$$

Here,

$$\rho_1^{(i)} = \frac{\eta_1^{(i)}(4\mu + 3\kappa)}{\kappa(4\mu + 3\eta_1^{(i)})}, \quad \rho_2^{(i)} = \frac{\eta_2^{(i)}}{\mu(1-\beta) + \beta\eta_2^{(i)}}, \quad \rho_3^{(i)} = \frac{\eta_3^{(i)}}{\mu(1-\beta) + \beta\eta_3^{(i)}} \tag{39}$$

and $$\eta_1^{(i)} = \tfrac{1}{3}(C_{11}^{(i)} + 2C_{12}^{(i)}), \quad \eta_2^{(i)} = \tfrac{1}{2}(C_{11}^{(i)} - C_{12}^{(i)}), \quad \eta_3^{(i)} = C_{44}^{(i)}, \tag{40}$$

where β is given by (26). The derivation of these formulas is given in the appendix. They simplify to comparable formulas given by Budiansky (1965) and Hill (1965*b*) when each phase is isotropic (i.e. $\eta_2^{(i)} = \eta_3^{(i)} \equiv \eta^{(i)}$) and to the Hershey–Kröner equations (22) and (23) for a single phase cubic polycrystal.

A self-consistent calculation of the initial yield surface leads to the maximum shear stress criterion just as in the case of the polycrystal. Equations (24) to (26) are still valid if ρ_2 and ρ_3 in (24) are associated with the values in (39) for the phase which yields first, that is, for the set $\rho_2^{(i)}$, $\rho_3^{(i)}$ and $\tau_y^{0(i)}$ which gives the smallest value $\bar{\tau}_y^0$ in (24). Details of this derivation are also discussed in the appendix.

Two special cases reveal the sort of effects which can be expected. Consider first a composite for which the first phase is isotropic with shear modulus μ_1 and an infinite bulk modulus and the second phase is made up of rigid spheres with volume concentration c_2. The macroscopic shear modulus from (38) is

$$\mu = \frac{\mu_1}{1 - \frac{5}{2}c_2} \tag{41}$$

and the initial yield criterion (24) becomes

$$\tfrac{1}{2}|\bar{\sigma}_{\mathrm{I}} - \bar{\sigma}_{\mathrm{III}}| = \frac{1 - c_2}{1 - \frac{5}{2}c_2}\tau_y^0, \tag{42}$$

where τ_y^0 is the critical yield stress for the crystals making up phase 1.

A second simple illustration occurs when phase 1 is isotropic with $\nu_1 = \frac{1}{5}$ and phase 2 is rigid. In this case,

$$\kappa = \frac{\kappa_1}{1 - 2c_2}, \quad \mu = \frac{\mu_1}{1 - 2c_2} \tag{43}$$

and

$$\tfrac{1}{2}|\bar{\sigma}_{\mathrm{I}} - \bar{\sigma}_{\mathrm{III}}| = \frac{1 - c_2}{1 - 2c_2}\tau_y^0. \tag{44}$$

The obvious limitations of the elastic results (41) and (43) at rigid inclusion concentrations approaching 40 and 50 %, respectively, have been discussed by Budiansky (1965) and Hill (1965*b*). Similar limitations are apparent in the initial yield predictions. The remarks in §2 on the effect of anisotropy in causing highly localized plastic strain at a stress level below that indicated by the self-consistent model apply here as well. In fact, it is even more transparent that a rigid inclusion in an isotropic matrix acts as a stress concentrater. Plastic yielding will occur in the immediate vicinity of certain regions on the surface of the inclusion at applied stresses below the level required if no inclusion were present and certainly below (42) or (44). However, here again it seems likely that the initial yield stress of the self-consistent model will play the role of a rather ill-defined effective yield stress demarking the onset of rapidly increasing plastic strain. In the early stages of the plastic deformation, anyway, the self-consistent calculation will underestimate the plastic strain.

According to this self-consistent calculation, initial yield depends only on the

concentration of the non-yielding inclusions, c_2, and in no way on the mean spacing between the inclusions. The present model has no bearing on particle hardened composites, such as those studied by Ashby (1966), for example, whose inclusions are microscopic in the sense that their size and/or spacing is on the order of the dislocation spacing within the crystal. Here the limitations of a continuum theory of crystal plasticity are inherently involved. For reasons similar to those discussed in conjunction with the polycrystal application, the yield stress of the crystal τ_y^0 must be regarded as its yield stress *in situ*.

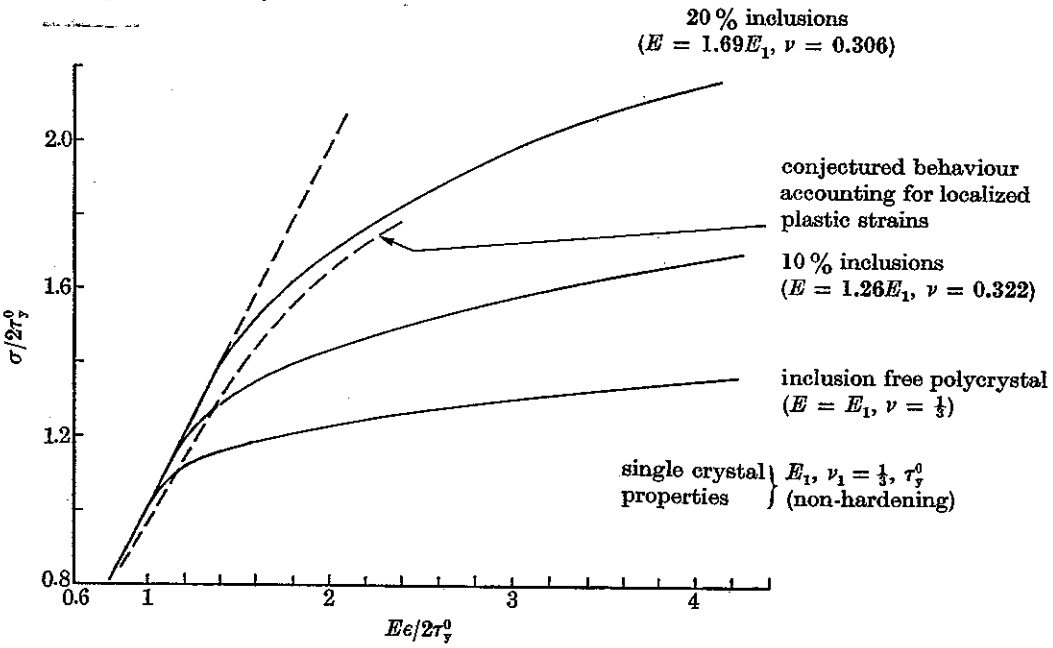

FIGURE 8. Tensile stress–strain curves for composites of rigid spherical inclusions and non-hardening, isotropic f.c.c. single crystals with random orientation.

If phase 2 is rigid, then $L_c^{(2)}A_c^{(2)} = L^* + L$ and (35) reduces to

$$L = (c_2/c_1)L^* + \{L_c^{(1)}A_c^{(1)}\}. \tag{45}$$

Thus, an elastic-plastic calculation for a composite of rigid inclusions interspersed with randomly orientated single crystals requires only a very minor modification of the previous polycrystal calculation.

Tensile stress–strain curves for such composites with isotropic f.c.c. single crystals are plotted in figure 8 for rigid inclusion concentrations of 0.1 and 0.2. For comparison the curve for an inclusion-free polycrystal is repeated from figure 1. The overall elastic properties from (38) are also recorded in this figure. Rigid inclusions harden the composite in the manner shown. Yet, consistent with our earlier discussion, the dashed curve should be typical of the actual behaviour for a concentration $c_2 = 0.2$ accounting for plastic straining which occurs prior to the yield value, $2\bar{\tau}_y^0$, predicted by the self-consistent model.

Appendix

(a) *Self-consistent calculation of the overall elastic moduli and initial yield surface of f.c.c. polycrystals and composites*

The general procedure for calculating the overall elastic moduli, which we now apply specifically to composites whose constituents have cubic symmetry, has been discussed in detail by Budiansky (1965), Hill (1965*a*, *b*) and Walpole (1969). Here only the major steps pertinent to arriving at (22), (23) and (38), which have already been introduced, will be recorded (following, as before, the notation used by Hill).

Let A_{ijkl} be the components of a fourth-order tensor ($A_{ijkl} = A_{ijlk} = A_{jikl} = A_{klij}$) with 'cubic symmetry' with respect to some set of axes. In the cubic axes, the components of $\boldsymbol{A}$ are completely specified if we write symbolically

$$\boldsymbol{A} \equiv (3\eta_1, 2\eta_2, 2\eta_3), \tag{46}$$

where $3\eta_1 = A_{1111} + 2A_{1122}$, $2\eta_2 = A_{1111} - A_{1122}$ and $2\eta_3 = 2A_{1212}$. Furthermore, with the definition (46) the inverse of $\boldsymbol{A}$ is given by

$$\boldsymbol{A}^{-1} \equiv \left(\frac{1}{3\eta_1}, \frac{1}{2\eta_2}, \frac{1}{2\eta_3}\right). \tag{47}$$

If $\boldsymbol{A}$ is isotropic, then $\eta_2 = \eta_3$ and we write $(3\eta_1, 2\eta_2, 2\eta_3) \equiv (3\eta_1, 2\eta_2)$.

Consider an N-phase composite with volume concentration c_i for the ith phase. A self-consistent equation for the overall elastic moduli is

$$\boldsymbol{L} = \sum_{i=1}^{N} c_i \{\boldsymbol{L}_c^{(i)} \boldsymbol{A}_c^{(i)}\}. \tag{48}$$

If each phase is randomly orientated, $\boldsymbol{L}$ is an isotropic tensor and is completely specified by the overall bulk modulus κ and shear modulus μ and $\boldsymbol{L} \equiv (3\kappa, 2\mu)$. The associated constraint tensor for spherical voids is also isotropic and is given by (see, for example, the next section of the appendix)

$$\boldsymbol{L}^* \equiv 2\mu\left(2, \frac{1-\beta}{\beta}\right), \tag{49}$$

where β is defined in (26). With respect to the cubic axes of the grain, $\boldsymbol{L}_c^{(i)}$ for the ith phase can be written in terms of the three independent elastic moduli (e.g. in the usual notation $L_{1111}^{(i)} = C_{11}^{(i)}$, $L_{1122}^{(i)} = C_{12}^{(i)}$ and $L_{1212}^{(i)} = C_{44}^{(i)}$) as

$$\boldsymbol{L}_c^{(i)} \equiv (3\eta_1^{(i)}, 2\eta_2^{(i)}, 2\eta_3^{(i)}), \tag{50}$$

where consistent with the definition (46) the η's are given in (40). Next, $\boldsymbol{A}_c^{(i)}$ and $\boldsymbol{B}_c^{(i)}$ are readily calculated in the grain axes using (37) with the results

$$\boldsymbol{B}_c^{(i)} \equiv (\rho_1^{(i)}, \rho_2^{(i)}, \rho_3^{(i)}) \quad \text{and} \quad \boldsymbol{A}_c^{(i)} \equiv (\kappa\rho_1^{(i)}/\eta_1^{(i)}, \mu\rho_2^{(i)}/\eta_2^{(i)}, \mu\rho_3^{(i)}/\eta_3^{(i)}), \tag{51}$$

where the ρ's were previously defined in (39).

The equally weighted average of the components of a tensor A over all orientations yields the components of an isotropic tensor so that

$$\{A\} \equiv (3\xi, 2\zeta) \quad \text{where } 9\xi = A_{iijj} \quad \text{and} \quad 10\zeta = A_{ijij} - \tfrac{1}{3}A_{iijj}. \tag{52}$$

If A has cubic symmetry and is denoted by (46) then $\xi = \eta_1$ and $\zeta = \frac{1}{5}(2\eta_2 + 3\eta_3)$.

Using (52) with (48) to (51) we obtain simultaneous equations for κ and μ:†

$$\sum_{i=1}^{N} c_i \rho_1^{(i)} = 1 \quad \text{and} \quad \sum_{i=1}^{N} c_i (2\rho_2^{(i)} + 3\rho_3^{(i)}) = 5. \tag{53}$$

To calculate the initial yield surface for a polycrystal or composite using the self-consistent model, we determine the minimum value of λ such that the applied overall stress $\lambda\bar{\boldsymbol{\sigma}}^0$ results in a resolved shear stress equal to, but not exceeding, τ_y^0 on at least one slip system for one grain orientation. The calculation will be carried out for a polycrystal, so as to avoid an encumbered notation, but the generalization of the resulting formulae to a multi-phase composite will be obvious.

Fix attention on an anisotropic f.c.c. grain with a given orientation and choose one of the 24 crystallographically identical slip systems whose normal m_i and slip direction n_i are defined relative to the grain axes by

$$m_i = \tfrac{1}{\sqrt{3}}[1, 1, 1], \quad n_i = \tfrac{1}{\sqrt{2}}[-1, 1, 0]. \tag{54}$$

The resolved shear stress τ on this system is

$$\tau = \boldsymbol{\sigma}_c \boldsymbol{\alpha} = \sigma_{cij} m_i n_j, \tag{55}$$

where by (14) $\boldsymbol{\sigma}_c = \lambda B_c \bar{\boldsymbol{\sigma}}^0$. Now use (51) to calculate τ for an orientation of the grain specified by the direction cosines l_{ij} relating the grain axes (i) to the axes (j) of the components of the overall applied stress, $\lambda\bar{\sigma}_{ij}^0$. The result is

$$\tau = \tfrac{\lambda}{\sqrt{6}}[\rho_2(-l_{1i}l_{1j} + l_{2i}l_{2j}) + \rho_3(-l_{1i}l_{3j} + l_{2i}l_{3j})]\bar{\sigma}_{ij}^0. \tag{56}$$

The critical grain orientation for a given $\lambda\bar{\boldsymbol{\sigma}}^0$ is associated with the set of direction cosines l_{ij} which minimizes τ.

To see that this calculation yields a modified maximum shear stress (Tresca) criterion, we consider the following trivial comparison calculation. Consider a slip system whose unit normal $\hat{m}_i$ and unit slip direction $\hat{n}_i$ are defined by

$$\hat{n}_i = \tfrac{1}{\sqrt{2}}[-1, 1, 0], \quad \hat{m}_i = \frac{1}{\sqrt{(2\rho_2^2 + \rho_3^2)}}[\rho_2, \rho_2, \rho_3], \tag{57}$$

with these components being defined with respect to axes orientated identically to the axes of the grain considered just above. The value $\hat{\tau}$ of $\lambda\bar{\boldsymbol{\sigma}}^0$ resolved on this slip system is

$$\hat{\tau} = \lambda \hat{m}_i \hat{n}_j l_{ip} l_{jq} \bar{\sigma}_{pq}^0, \tag{58}$$

and when this expression is expanded out using (57) it becomes exactly (56) except for a relative factor

$$\left(\frac{3}{2\rho_2^2 + \rho_3^2}\right)^{\frac{1}{2}}. \tag{59}$$

† Other forms of these equations can be obtained just as for the case of isotropic phases as discussed by Budiansky (1965) and Hill (1965*b*) and in the general case by Hill (1965*a*).

Minimization of $\hat{\tau}$ with respect to all l_{ij} for a given $\lambda\overline{\sigma}^0_{ij}$ obviously leads to a maximum shear stress criterion and if λ is picked so that $\hat{\tau} = \tau^0_y$ then

$$\tfrac{1}{2}\lambda|\overline{\sigma}^0_{\rm I} - \overline{\sigma}^0_{\rm III}| = \tau^0_y. \tag{60}$$

Thus it follows that a maximum shear stress condition holds for the polycrystal, as well, but instead with the factor (59) multiplying τ^0_y in (60) or as given previously in the form (24).†

(*b*) L^* *for general anisotropy and transverse isotropy for spherical voids*

Here we record without derivation formulas for the constraint tensor $\boldsymbol{L}^*$ for spherical voids which was introduced in §2. Eshelby's (1961) tensor $\boldsymbol{S}$ arises naturally in the solution to this boundary-value problem in anisotropic elasticity. Let a spherical inclusion, whose elastic moduli $\boldsymbol{L}$ are identical to those of the unbounded matrix undergo a uniform stress-free transformation strain $\boldsymbol{\epsilon}^T$. The total resulting strain $\boldsymbol{\epsilon}^c$ in the inclusion constrained by the matrix is uniform and is related to the transformation strain by $\boldsymbol{\epsilon}^c = \boldsymbol{S}\boldsymbol{\epsilon}^T$. Hill's (1965*a*) tensor $\boldsymbol{L}^*$ is related to $\boldsymbol{S}$ by

$$\boldsymbol{L}^*\boldsymbol{S} = \boldsymbol{L}(\boldsymbol{I}-\boldsymbol{S}). \tag{61}$$

Kneer (1965) has derived formulas for $\boldsymbol{S}$ but in checking his results we have uncovered several errors or misprints in his specialized formulas for transverse isotropy. For this reason, and because of certain ambiguities in the way Kneer's formulas have been presented, it seems well worth while to relist these formulas and to note the discrepancies. For details of the method of solution the reader is referred to Kneer's paper.‡

In Cartesian components, $\quad S_{ijkl} = \Lambda_{ijmn}L_{mnkl}, \tag{62}$

where

$$\Lambda_{ijmn} = \frac{1}{16\pi}\int_0^{\pi}\sin\theta\,\mathrm{d}\theta\int_0^{2\pi}\mathrm{d}\phi(\hat{U}_{im}k_nk_j + \hat{U}_{jm}k_nk_i + \hat{U}_{in}k_mk_j + \hat{U}_{jn}k_mk_i). \tag{63}$$

In the above equation $\hat{U}_{ij}(=\hat{U}_{ji})$ satisfies

$$L_{ijkl}\hat{U}_{km}k_jk_l = \delta_{im}, \tag{64}$$

with $k_1 = \sin\theta\cos\phi$, $k_2 = \sin\theta\sin\phi$ and $k_3 = \cos\theta$. Note that

$$\Lambda_{ijmn} = \Lambda_{jimn} = \Lambda_{ijnm} = \Lambda_{mnij};$$

but for general anisotropy the first and last pairs of indices of S_{ijkl} will not necessarily be interchangeable.

A numerical evaluation of the double integration in (63) is a practical possibility. However, Kneer (1965) has shown that this double integration can be reduced to formulas involving only well-behaved ordinary integrals for the case of transverse

† The observation that a self-consistent calculation yields a modified Tresca condition was communicated to the author by R. Hill in late 1967. Subsequently, a derivation of (24) alternative to the one given above was set as a question on a part III course of the Cambridge Tripos.

‡ The general procedure in arriving at (63) is also given in an unpublished manuscript by J. R. Willis.

isotropy. With the 3 axis identified as the axis of symmetry so that the 6×6 matrix (28) of moduli L_{ij} is appropriate, (63) reduces to

$$A_{ijkl} = \sum_{m=0}^{3} K^{(m)} A^{(m)}_{ijkl}, \tag{65}$$

where

$$K^{(m)} = \frac{1}{8}\int_0^1 \frac{z^{2m}\,dz}{a_0 + a_1 z^2 + a_2 z^4 + a_3 z^6} \quad (m = 0, 3), \tag{66}$$

and where the a's and the nonzero $A^{(k)}$'s are given in table 1.† Each of the $A^{(k)}$'s has the same symmetry in its indices as A as noted in the table.

For complete isotropy,

$$S_{ijkl} = (1 - \tfrac{5}{3}\beta)\delta_{ij}\delta_{kl} + \tfrac{1}{2}\beta(\delta_{ik}\delta_{jl} + \delta_{il}\delta_{jk} - \tfrac{2}{3}\delta_{ij}\delta_{kl})$$

and

$$L^*_{ijkl} = \tfrac{4}{3}\mu\delta_{ij}\delta_{kl} + ([1-\beta]/\beta)\mu(\delta_{ik}\delta_{jl} + \delta_{il}\delta_{jk} - \tfrac{2}{3}\delta_{ij}\delta_{kl}),$$

where β is given by (26).

(c) *Numerical method*

A broad outline of the numerical procedure is given in § 2 and some further details are filled in here. As described in § 2, the iterative procedure for calculating $\boldsymbol{L}$ (associated with a prescribed stress or strain rate) involved calculating $\boldsymbol{L}_c$ and then $\boldsymbol{A}_c$ for each grain and improving the estimate of $\boldsymbol{L}$ by using (20) or (45). This iteration is repeated until adequate convergence is achieved. The efficiency of this procedure is greatly improved if there are several sub-iterations within each iteration in which the $\boldsymbol{L}_c$'s are not recalculated but only the $\boldsymbol{A}_c$'s and the improved estimates of $\boldsymbol{L}$. Convergence is quite rapid even when there is an abrupt change in the 'direction' of prescribed stress or strain rate as in the case of the calculations associated with figures 6 and 7. In that calculation three iterations, with four sub-iterations within each iteration, was more than adequate to ensure convergence.

Since no preferred orientation of the grains of either the polycrystal or the composite was assumed, averages over all the grains could be replaced by an equally weighted average over all the orientations. Numerical results were obtained by considering a finite set of orientations corresponding to discrete values of the Euler angles relating the axes of the grain to those of the specimen. Because of the symmetry it was only necessary to allow each Euler angle to cover the interval from 0 to $\frac{1}{2}\pi$. In all the tensile calculations each of the three intervals was divided into six equally spaced stations resulting in a total of 216 orientations. Advantage was taken of the invariance of the properties of the grain with respect to rotations about the tensile direction and thus $\boldsymbol{L}_c$ was calculated independently only for 36 orientations. For the corner calculations on figures 6 and 7, it was necessary to obtain $\boldsymbol{L}_c$ and $\boldsymbol{A}_c$ for all the orientations and for these calculations a total of only 64 orientations was

† Kneer's (1965) equivalent expression for a_2 has an incorrect sign on the first term. This is clearly a misprint since our numerical results for the integrals (66) check his. There is also a difference in one of the terms of $A^{(2)}_{1313}$ and in three of the terms of $A^{(3)}_{1313}$. Kneer's expressions as printed do not check for the case of complete isotropy.

TABLE 1

$$a_0 = L_{11}L_{44}L_{66}$$

$$a_1 = -3L_{11}L_{44}L_{66}+L_{11}L_{33}L_{66} -L_{13}^2L_{66}-2L_{13}L_{44}L_{66}+L_{11}L_{44}^2$$

$$a_2 = 3L_{11}L_{44}L_{66}+L_{11}L_{33}L_{44} +L_{33}L_{44}L_{66}-L_{13}^2L_{44}-2L_{13}L_{44}^2 -2L_{11}L_{33}L_{66}-2L_{11}L_{44}^2+2L_{13}^2L_{66} +4L_{13}L_{44}L_{66}$$

$$a_3 = -L_{11}L_{44}L_{66}+L_{33}L_{44}^2 -L_{11}L_{33}L_{44}-L_{33}L_{44}L_{66} +L_{13}^2L_{44}+2L_{13}L_{44}^2+L_{11}L_{33}L_{66} +L_{11}L_{44}^2-L_{13}^2L_{66}-2L_{13}L_{14}L_{66}$$

$$\Lambda^{(0)}_{1111} = L_{44}(L_{11}+3L_{66})$$

$$\Lambda^{(1)}_{1111} = (L_{11}+3L_{66})(L_{33}-3L_{44}) -(L_{13}+L_{44})^2+4L_{44}^2$$

$$\Lambda^{(2)}_{1111} = (3L_{44}-2L_{33})(L_{11}+3L_{66}) +4L_{33}L_{44}-8L_{44}^2+2(L_{13}+L_{44})^2$$

$$\Lambda^{(3)}_{1111} = (L_{33}-L_{44})(L_{11}+3L_{66}-4L_{44}) -(L_{13}+L_{44})^2$$

$$\Lambda^{(0)}_{1122} = -L_{44}(L_{11}-L_{66})$$

$$\Lambda^{(1)}_{1122} = (3L_{44}-L_{33})(L_{11}-L_{66}) +(L_{13}+L_{44})^2$$

$$\Lambda^{(2)}_{1122} = (2L_{33}-3L_{44})(L_{11}-L_{66}) -2(L_{13}+L_{44})^2$$

$$\Lambda^{(3)}_{1122} = (L_{44}-L_{33})(L_{11}-L_{66}) +(L_{13}+L_{44})^2$$

$$\Lambda^{(0)}_{1133} = 0$$

$$\Lambda^{(1)}_{1133} = -4L_{66}(L_{13}+L_{44})$$

$$\Lambda^{(2)}_{1133} = 4(2L_{66}-L_{44})(L_{13}+L_{44})$$

$$\Lambda^{(3)}_{1133} = 4(L_{44}-L_{66})(L_{13}+L_{44})$$

$$\Lambda^{(0)}_{3333} = 0$$

$$\Lambda^{(1)}_{3333} = 8L_{11}L_{66}$$

$$\Lambda^{(2)}_{3333} = -16L_{11}L_{66}+8L_{44}(L_{11}+L_{66})$$

$$\Lambda^{(3)}_{3333} = 8(L_{11}-L_{44})(L_{66}-L_{44})$$

$$\Lambda^{(0)}_{1313} = L_{11}L_{66}$$

$$\Lambda^{(1)}_{1313} = 2L_{11}L_{44}-2L_{13}L_{66}-3L_{11}L_{66}$$

$$\Lambda^{(2)}_{1313} = L_{11}L_{13}+L_{33}L_{66}-4L_{11}L_{44} +L_{44}^2-(L_{13}+L_{44})^2+4L_{13}L_{66} -2L_{13}L_{44}+3L_{11}L_{66}$$

$$\Lambda^{(3)}_{1313} = -L_{11}L_{33}-L_{33}L_{66}+2L_{33}L_{44} +2L_{11}L_{44}-L_{44}^2+(L_{13}+L_{44})^2 -2L_{13}L_{66}+2L_{13}L_{44}-L_{11}L_{66}$$

$$\Lambda_{2222} = \Lambda_{1111};\ \Lambda_{2233} = \Lambda_{1133};\ \Lambda_{2323} = \Lambda_{1313};\ \Lambda_{1212} = \tfrac{1}{2}(\Lambda_{1111}-\Lambda_{1122});\ \Lambda_{ijkl} = \Lambda_{jikl} = \Lambda_{ijlk} = \Lambda_{klij}.$$

used. Accordingly, these are the least accurate of results given. Moduli were calculated at ten values of θ to obtain the plots of figures 6 and 7.

Between 15 and 30 incremental steps were taken in the calculation of the tensile stress–strain curves. By far the best check on the accuracy of the procedure was obtained by recalculating the tensile curve for the K.B.W. model, as described in §4, and comparing it with the highly accurate calculations of Budiansky & Wu (1962) or Hutchinson (1964). With 216 orientations the agreement was excellent and the curves of stress against plastic strain were virtually indistinguishable in a plot such as figure 4. Further, a calculation, based on this procedure with 216 orientations, of the elastic shear modulus of a polycrystal whose crystals have the anisotropy of copper (29) leads to a result which is accurate to three significant figures compared to the prediction of (23).

The subsequent yield surfaces of figure 5 were calculated in a straightforward way. At any value of the tensile stress it is a simple matter to determine if the stress state $(\bar{\sigma}_{13}, \bar{\sigma}_{33})$ or $(\bar{\sigma}_{12}, \bar{\sigma}_{33})$ lies within the elastic region or not and the bounding surface of the elastic region is readily obtained.

Finally, we mention in passing that Hill's model, like the Lin and K.B.W. models, predicts that after a tensile strain of about $(E\epsilon/2\tau_y^0) = 5$ the response of an f.c.c. polycrystal is not purely elastic when the tensile load is decreased. In fact, a few of the slip systems in some of the grains continue to remain active and contribute a very small amount of plastic deformation in much the same manner as has been discussed by Hutchinson (1964) for the K.B.W. model. This effect is quite small but, strictly speaking, the models predict that the elastic region actually ceases to exist if the plastic strains are large enough and single crystal hardening is not overly high.

References

Ashby, M. F. 1966 *Phil. Mag.* **14**, 1157.
Batdorf, S. B. & Budiansky, B. 1949 *NACA TN* 1871.
Bishop, J. F. W. & Hill, R. 1951 *Phil. Mag.* **42**, 414, 1298.
Budiansky, B. 1965 *J. Mech. Phys. Solids* **13**, 223.
Budiansky, B., Hashin, Z. & Sanders, J. L. 1960 *Plasticity. Proc. 2nd Symp. on Naval Structural Mech.* p. 239. Pergamon Press.
Budiansky, B. & Wu, T. T. 1962 *Proc. 4th Congr. Appl. Mech.*, p. 1175.
Eshelby, J. D. 1957 *Proc. Roy. Soc. Lond.* A **241**, 376.
Eshelby, J. D. 1961 *Progress in solid mechanics*, vol. II. Amsterdam: North-Holland.
Hershey, A. V. 1954 *J. appl. Mech.* **21**, 236.
Hill, R. 1965*a* *J. Mech. Phys. Solids* **13**, 89.
Hill, R. 1965*b* *J. Mech. Phys. Solids* **13**, 213.
Hill, R. 1966 *J. Mech. Phys. Solids* **14**, 95.
Hill, R. 1967 *J. Mech. Phys. Solids* **15**, 79.
Hutchinson, J. W. 1964 *J. Mech. Phys. Solids* **12**, 11, 25.
Kneer, G. 1963 *Phys. Stat. Sol.* 3, K331.
Kneer, G. 1965 *Phys. Stat. Sol.* **9**, 825.
Kocks, U. F. 1970 *Metallurgical Trans.* **1**, 1121.
Koiter, W. T. 1953 *Q. appl. Math.* **11**, 350.
Koiter, W. T. 1960 *Progress in Solid Mechanics*, vol. I. Amsterdam: North-Holland.
Kröner, E. 1958 *Z. Phys.* **151**, 504.

Kröner, E. 1961 *Acta Metall.* **9**, 155.
Lin, T. H. 1957 *J. Mech. Phys. Solids* **5**, 143.
Mandel, J. 1965 *Int. J. Solids Struct.* **1**, 273.
Sanders, J. L. 1954 *Proc. 2nd U.S. Nat. Congr. Appl. Mech.* p. 455.
Taylor, G. I. 1938 *J. Inst. Metals* **62**, 307.
Taylor, G. I. & Elam, C. F. 1923 *Proc. Roy. Soc. Lond.* **A102**, 643.
Walpole, L. J. 1969 *J. Mech. Phys. Solids* **17**, 235.
Wu, T. T. 1966 *Int. J. Solids Struct.* **2**, 1.